UNSTEADY EFECTS IN SAND TRANSPORT UNDER NONLINEAR WAVES

P. A. Silva[1], T. Abreu[2] and F. Sancho[3]

Abstract

The phase-lag between the sediment concentration and the flow velocity in oscillatory flows determine, in certain circumstances, the magnitude and direction of cross-shore sediment transport. These unsteady effects depend on the characteristics of the wave induced motion (amplitude of the near-bed orbital velocity, wave period and non-linearity) and also on the bed sediment grain size distribution. This communication addresses this issue and proposes an analytical function that describes phase-lag effects. Net transport rates computed from quasi-steady formulations provide better estimates when the function is considered. Finally, the way how phase-lag effects induce changes in net transport rates under non-linear waves is further investigated.

1. Introduction

The phase-lag between the orbital velocity and sediment concentration in oscillatory flows is a process that affects the magnitude and direction of the cross-shore net sediment transport. The importance of unsteady phase-lag effects in sediment transport can be observed from the analysis of detailed measurements of flow velocities and sediment concentrations near the bed. The experiments of Watanabe and Isobe (1990) performed with ripple beds evidence that, in some conditions, an oscillatory flow leads to net sediment transport rates in the opposite direction of the mean current. These effects are due to the vortices formed over a ripple, either during the onshore or offshore motions. The vortices retain large amounts of sediment which were picked up from the bed and remain in suspension even when the magnitude of the velocity decreases at flow reversal phases. As a consequence, the sediment particles entrained into suspension during the positive half cycle (onshore velocities) are available to be transported in the opposite direction by the negative (offshore) velocities. These so-called unsteady effects, when the sediment concentration is not in phase with the flow motion, can be responsible for an offshore net sediment transport even when the waves propagate onshore. Whilst these phenomena can be easily observed over rippled bed oscillatory motions, they are also manifested even when the bed is flat, when intense sediment transport occurs in a so-called sheet flow layer (e.g., Dohmen-Jansen *et al.*, 2002; Silva *et al*., 2009; O'Donoghue and Wright, 2004; Ruessink *et al*., 2012).

The sheet flow layer is a near-bed layer with thickness of the order of mm to cm, and sand concentrations reach values between 200g/l to near 1600 g/l at the stationary bed. As an example, Figure 1 illustrates the development of the sheet flow layer during a wave cycle. These data were obtained from direct measurements of flow velocities and sediment concentrations near the bed in combined oscillatory and collinear current flows (see Silva *et al*., 2009, for details). As the velocity increases from zero, at each flow reversal, sediment particles are mobilized from the bed, thus causing local erosion associated with a deepening of the bed level and an increase in the erosion depth. These particles are entrained into the flow above the initial bed level causing an increase of sediment concentration at those levels and, consequently, raising the top level of the sheet flow layer. When the magnitude of the velocity decreases, the processes that sustain the sediment particles, either in the sheet flow or in the suspension layers, tend to vanish and sediment particles have a tendency to settle down to the bed, causing a decrease in the sheet flow layer thickness.

[1] University of Aveiro & CESAM, Campus Universitário de Santiago, 3810-193, Aveiro, Portugal. psilva@ua.pt
[2] Polytechnic Institute of Viseu & CESAM, ESTGV Campus de Repeses, 3504-510, Viseu, Portugal. tabreu@estv.ipv.pt
[3] LNEC – National Laboratory for Civil Engineering, Av. do Brasil, 101, 1700-066 Lisbon, Portugal. fsancho@lnec.pt

However, it is evident that the sheet flow layer does not vanish at the off-onshore flow reversal ($\omega t \approx 0°$) as it does at the opposite on-offshore ($\omega t \approx 180°$) flow reversal. This supports the existence of phase-lag effects between the sediment particles and the flow.

The presence of unsteady effects in sediment transport has been shown to become more significant for fine sediments (d_{50}<0.2 mm), small wave periods (e.g., Dohmen-Janssen, 1999; Dong *et al.*, 2013) and under nonlinear waves with skewed and asymmetric velocities (O'Donoghue and Wright, 2004; Ruessink *et al.*, 2012).

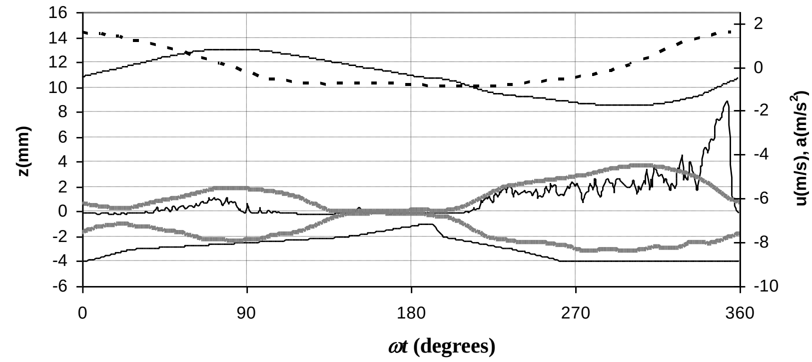

Figure 1. Time variation of the lower and upper levels of the sheet flow layer estimated from two independent measurements (black and grey solid lines at the lower part of the figure). The corresponding free-stream velocity and acceleration time series are shown by the upper solid and dashed curves, respectively (adapted from Silva *et al*., 2009).

Different empirical or theoretical transport formulas (e.g., quasi-steady and semi-unsteady models) are presently being used in order to predict sediment transport in coastal zones. Quasi-steady models (e.g., Bailard, 1981; Nielsen, 2006) assume that sand transport reacts immediately to changes in flow conditions: the instantaneous sediment transport is computed as a function of the bottom shear stress or the near bed velocity. The semi-unsteady models take into account the unsteady phase-lag effects by involving parameters that quantify the amount of sediment mobilized from the bed during a half-wave cycle and the sediment fall velocity (e.g., Dibajnia and Watanabe, 1992; Dohmen-Jansen *et al*., 2002; Dibajnia and Sato, 2004; Silva *et al*., 2006; van der A *et al*., 2013). Although these semi-unsteady models do not describe in detail the vertical distribution of the flow and sediment concentration, they overcome some deficiencies of the quasi-steady models.

This paper presents an analytical function that reflects the effect of phase-lags in net transport rates. The methodology follows the work of Silva *et al*. (2006) and is validated with a large dataset of net transport rates measured under non-linear waves in sheet flow conditions. The comparison between the predicted and experimental results allows to establish under which hydraulic conditions unsteady effects are important. Moreover, the effectiveness of the proposed function to provide better estimates of the net transport rates is assessed. At the end the limitations and advantages of the present non-steady function are discussed.

2. Methodology

According to Silva *et al*. (2006), the net transport rate¸ q_s, is computed by:

$$\frac{q_s}{\sqrt{(s-1)gd_{50}{}^3}} = \alpha \left|\Gamma\right|^{\beta} \frac{\Gamma}{\left|\Gamma\right|}, \tag{1}$$

with

$$\Gamma = \frac{u_c T_c (\Omega_c{}^3 + \Omega_t'^3) - u_t T_t (\Omega_t{}^3 + \Omega_c'^3)}{2(u_c T_c + u_t T_t)} \tag{2}$$

In these equations $s = \rho_s / \rho$, where ρ and ρ_s are the water and sediment density, respectively, g is the gravitational acceleration, T_c and T_t are the time duration of the positive and negative half cycle of the near bed velocity, respectively, with equivalent velocities u_c and u_t (the subscript c stands for crest and t for trough) (see Figure 2). The quantities Ω_i and Ω_i' ($i = c, t$) represent the amount of sediment that is entrained, transported and settled in the i half cycle, and the amount of sediment still in suspension from the i half cycle that will be transported in the next half cycle, respectively. Therefore, in Equations (1) and (2), q_s is computed from the difference between the sediment transported during the positive and negative half cycles of the oscillatory motion. The unsteady effects are taken into account through the exchange of sediment flux between successive half cycles. For example, if the ratio, ω_c, between the settling time of the sediment particles, T_{fall}, and the duration of the positive half cycle, T_c, is larger than a critical value, ω_{cr}, then $\Omega_c = \theta_c\ (\omega_{cr}/\omega_c)$ and $\Omega_c' = \theta_c\ (1\text{-}\omega_{cr}/\omega_c)$. Otherwise, $\Omega_c = \theta_c$ and $\Omega_c' = 0$. Here, θ_c represents the equivalent Shields parameter for the positive half cycle. The same reasoning is applied for the negative half cycle. T_{fall} is computed from the ratio between the height to which a particle is entrained into the flow, Δ_s, the sediment fall velocity and the parameter ω_{cri}, which is a function of the maximum Shields parameter. According to this model, Δ_s and ω_{cr} are mandatory for the existence of unsteady effects. It is noticed that Δ_s is proportional to the equivalent velocity for each half cycle (Dibajnia and Watanabe, 1992). Finally, the parameters α and β in Equation (1) are two empirical constants (α= 3.2 and β= 0.55).

In this work we investigate the sensitivity of the numerical solution in ω_{cr} by considering two different expressions: one proposed by Dibajnia (1995) and another by Silva *et al*. (2006).

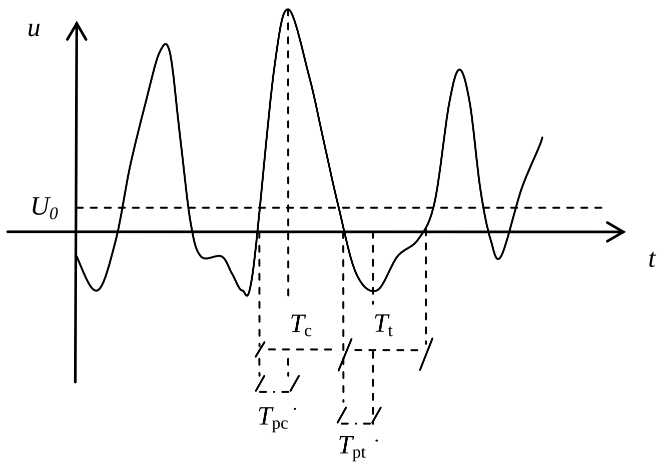

Figure 2. Near-bed time velocity series and definition of the T_c and T_t. U_0 represents the velocity of a mean current collinear with the oscillatory flow.

We can rewrite Equation (1) as a product of two functions:

$$q_s = F\, q_{sN} \ , \tag{3}$$

where q_{sN} represents the quasi-steady approach solution when phase-lag effects are not considered and F is a function that reflects the effect of the unsteady processes in sediment transport. An expression for q_{sN} can be derived from Equation (2) assuming that the primed quantities, Ω_i', are zero:

$$\frac{q_{sN}}{\sqrt{(s-1)gd_{50}{}^3}} = \alpha \left|\Gamma_N\right|^{\beta} \frac{\Gamma_N}{\left|\Gamma_N\right|}, \tag{4}$$

with

$$\Gamma_N = \theta_c{}^3 \frac{1-\alpha_o{}^7 \delta_o \gamma_0{}^3}{2(1+\alpha_o \delta_o)} \ . \tag{5}$$

It results that *F* is given by:

$$F = \left|G\right|^{\beta} \frac{G}{\left|G\right|}, \tag{6}$$

with

$$G = \frac{Z_c{}^3 + \alpha_o{}^6 (1-Z_t)^3 \gamma_0{}^3 - \alpha_0{}^7 \delta_o \gamma_0{}^3 \, Z_t{}^3 - \alpha_0 \delta_o (1-Z_c)^3}{1-\alpha_o{}^7 \delta_o \gamma_0{}^3} \ . \tag{7}$$

The quantities Z_c , Z_t , α_o, δ_o and γ_o in Equations (5) and (7) are given by:

$$Z_c = \frac{\omega_{cr}}{\omega_c}; \quad Z_t = \frac{\omega_{cr}}{\omega_t}; \quad \gamma_o = \frac{\theta_t}{\theta_c}; \quad \alpha_o = \frac{u_t}{u_c}; \quad \delta_o = \frac{T_t}{T_c}; \tag{8}$$

As stated before, when $\omega_{cr} > \omega_c$ and/or $\omega_{cr} > \omega_t$ (the exchange mechanism is not effective) the values of Z_c and/or Z_t in Equation (7) are set equal to one. According to Equation (6), the sign of *F* depends on the sign of *G*. Therefore, these unsteady effects may also change the direction of the net transport rate.

3 Results

The net transport rates q_s, q_{sN} and the values of the function *F* in Equations (3)-(7) are evaluated for a large data set corresponding to non-linear oscillatory flows in the sheet flow regime. The estimated values are compared with the measurements. The dataset comprises different velocity skewed and asymmetric oscillatory flows with and without the presence of collinear currents. In the following, OD04 stands for O'Donoghue and Wright (2004); WS04 for Watanabe and Sato (2004); S11 for Silva *et al*. (2011); and D13 for Dong *et al*. (2013) data (see Table 1). All the experiments were performed in oscillating flow tunnels. The velocity time series input corresponding to each experimental condition was synthetized from Abreu *et al*. (2010) formulation. According to this formulation the value of two parameters *r* and ϕ must be prescribed: *r* is a parameter that reflects the index of skewness or nonlinearity (r =0 corresponds to a sinusoidal wave) and ϕ a wave form parameter (the orbital velocity is asymmetric for $\phi = 0$, as in a saw-tooth wave profile, skewed for $\phi = -\pi/2$, as in a first order cnoidal wave, and mixed asymmetric-skewed for $-\pi/2 < \phi < 0$. The values of *r* and ϕ were found as described in Abreu *et al*. (2010). The equivalent Shields parameter for the positive and negative half-cycles (θ_c, θ_t) in Equations (5) and (7) were computed from the amplitude of the orbital velocity, U_w, and the friction factors following Silva *et al*. (2006). The maximum Shields parameter for the estimation of ω_{cr} was computed from Abreu *et al*.'s (2013a) formulation.

Figure 3 shows the computed and measured net transport rates for the whole data set. Figure 3a) shows the quasi-steady solution (Equations 4 and 5); whereas in Figure 3b) the values of ω_{cr} were computed following Silva *et al*. (2006) and in Figure 3c) according to Dibajnia (1995). In the sheet flow regime, ω_{cr} is constant for the Dibajnia (1995) model. In the present computations, it results ω_{cr} =0.9. For Silva *et al*. (2006) formulation ω_{cr} changes with the maximum Shields parameter.

Table 1. Overview of the data set

	U_w (m/s)	T(s)	r	ϕ	U_0 (m/s)	d_{50} (mm)	nº tests
OD04	~1.2	4; 5; 6; 7.5	0.49	$-\pi/2$	0	0.15; 0.28; 0.51	8
WS04	0.7 – 1.6	3; 5	0.2 – 0.6	*0*	0 ; -0.1 ; -0.2	0.2; 0.74	52
VA10	0.85 – 1.34	5; 6; 7; 9	0.15– 0.6	*~0*	0	0.15; 0.27; 0.46	35
S11	~1.25	7; 10	0.27 – 0.45	*0 ; ~* $-\pi/2$	0 ; -0.2 ; -0.4	0.2	11
D13	0.6 – 1.4	3; 5; 6; 7	0.16 – 0.7	$-\pi/2 < \phi < 0$	0 ; -0.3 ; -0.5	0.16; 0.2; 0.3	53

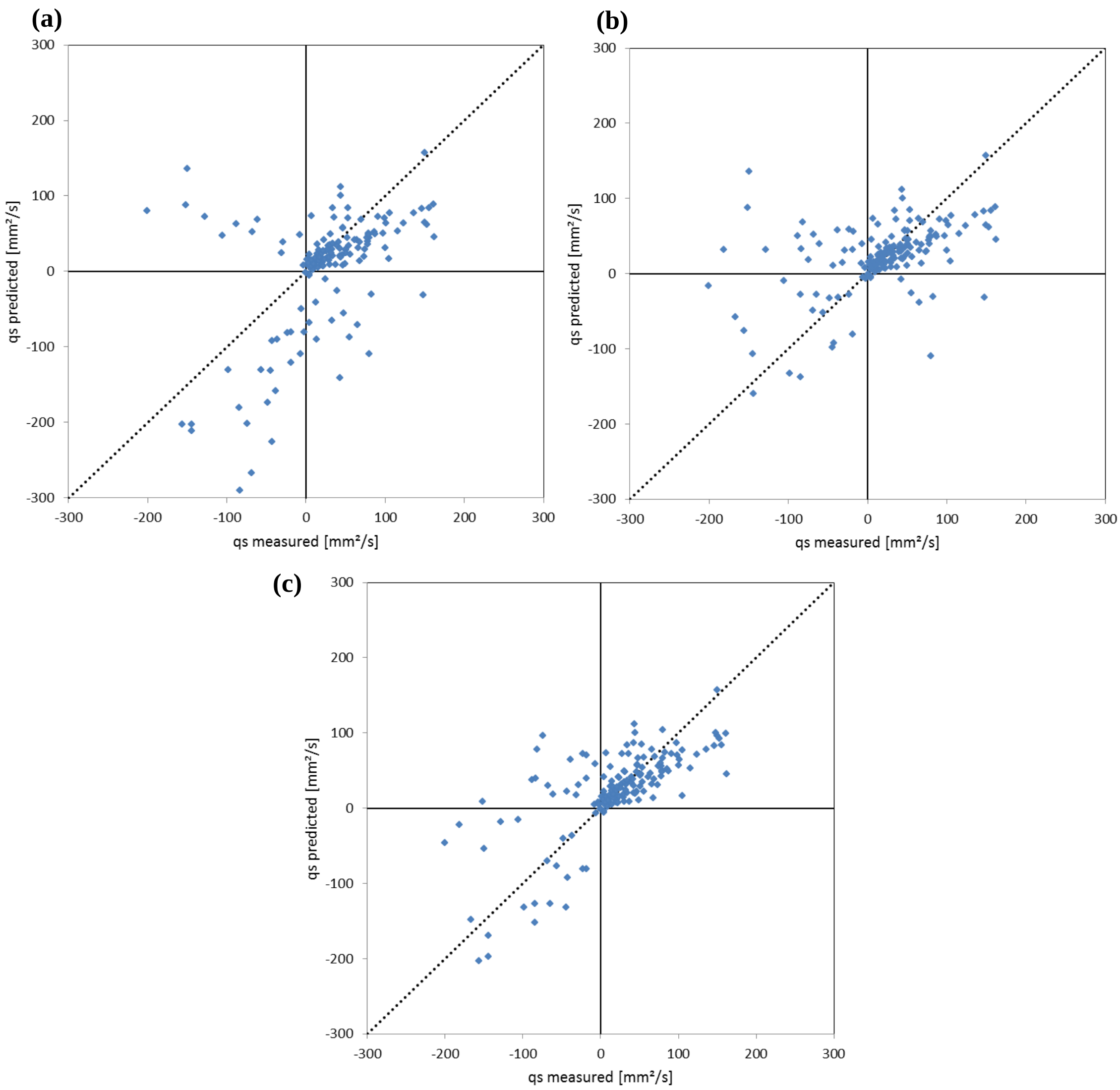

Figure 3. Measured against predicted net transport rates (Silva *et al.*, 2006): a) quasi-steady solution, (q_{sN}); b) q_s with ω_{cr} computed from Silva *et al.* (2006); c) q_s with ω_{cr} computed from Dibajnia (1995).

The results show that:

- For approximately 40% of the test conditions, the inclusion of unsteady effects (by means of Eq. 7) lead to an exchange of sediments between successive half cycles that change the magnitude and, in some cases, the direction of the quasi-steady net transport rates. 60% of these cases correspond to the hydraulic conditions of WS04 and D13 performed with T=3s and large negative velocities.
- The values of G in Equation (7) depend on the value of ω_{cr} considered. This dependency is more evident for the subset of WS04 and D13 data pointed above, as can be seen by comparing the results for the negative measured q_s in Figures 3b) and 3c). The variation of ω_{cr} with the Shields parameter as proposed by Silva *et al*. (2006) seams to overpredict the phase-lag effects. In general, for the other experimental conditions small changes were reported.
- The prediction of net transport rates improved when the correction of non-steady effects was considered. The performance of the model in terms of the root mean square error (RMSE) decreases from 1.62 to 0.70 from Figure 3a) to Figure 3c). The corresponding values for the dataset of D13 are 1.93 and 0.73.

The efficiency of the analytical function F to correct net transport rates estimated from other quasi-steady sediment transport models is depicted in Figure 4 for the Abreu *et al*. (2013a) formulation. Only the D13 dataset is considered here (see the companion paper of Abreu *et al*., 2013b). The Dibajnia (1995) formulation to compute ω_{cr} was considered. It is seen that an overall improvement of the net transport rates is achieved: the RMSE decrease from 0.92 to 0.65.

The analytical function F also provides an insight on how the unsteady effects determine the net transport rates in non-linear waves. With this purpose, q_s was computed from Equations (3) - (7) considering as input skewed and asymmetric orbital velocities time series synthetized by Abreu *et al*.'s (2010) formulation. The following values were assumed: U_w = 1.5 m/s and T = 7s by changing r (0 – 0.8) and keeping ϕ, the waveform parameter, constant (ϕ = 0) or by changing ϕ (-π/2 – 0) and keeping r constant (r = 0.5). In every case, d_{50} = 0.2mm and U_0 = 0. Figures 5 and 6 show the computed net transport rates as a function of the variable parameter (r or ϕ) for the quasi-steady and semi-unsteady model. For certain values of r and ϕ the orbital velocity and the bed shear stress time series (the latter computed from Abreu *et al*., 2013a) are shown. In Figure 5, changing r implies changing the wave form from sinusoidal (A: r=0) to a saw-tooth shape with increasing asymmetry (B: r=0.8). The unsteady effects become larger as the nonlinearity parameter r increases and they contribute to an increase of the amount of sediment that is transported in the wave direction (F is positive and larger than 1). This is attributed to a relatively small time allowed for sediments to settle in the negative half cycle which decrease as T_{pt} increases (see Figure 1 for the definitions of T_{pt}).

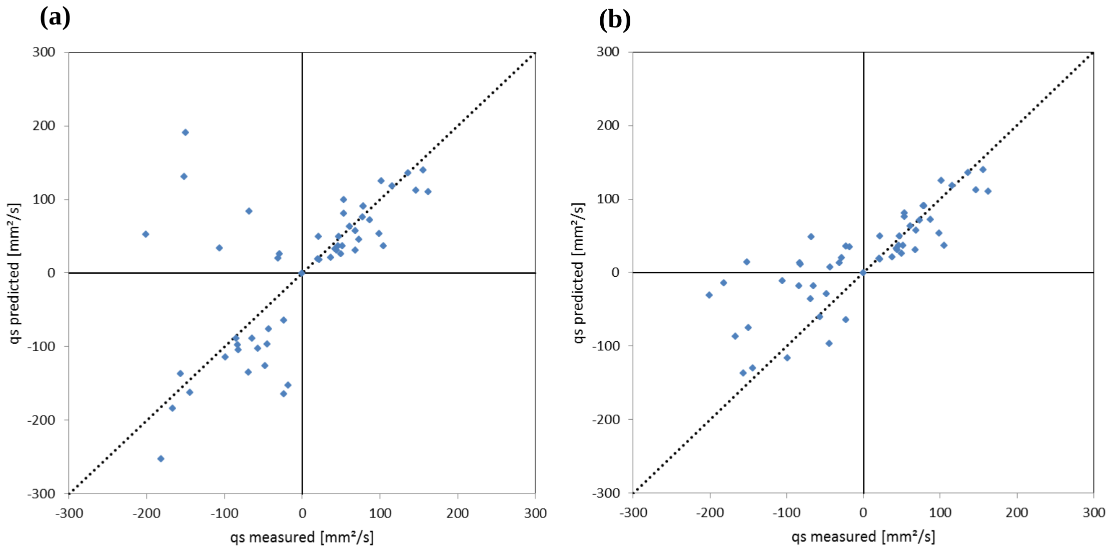

Figure 4. Measured against predicted (q_s) net transport rates (D13 dataset): Abreu *et al*. (2013a) standart model; b). Abreu *et al*. (2013) standart model corrected by the *F* function.

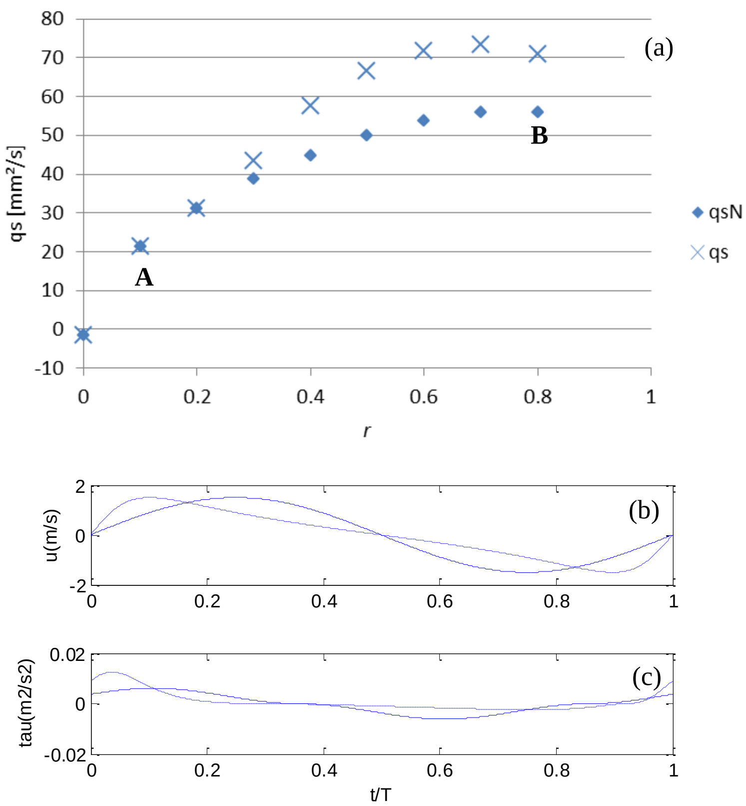

Figure 5. (a) Computed q_{sN} and q_s against *r*; b) time series of the orbital velocity and c) bed-shear stress corresponding to **A** (solid line) and **B** (dashed line).

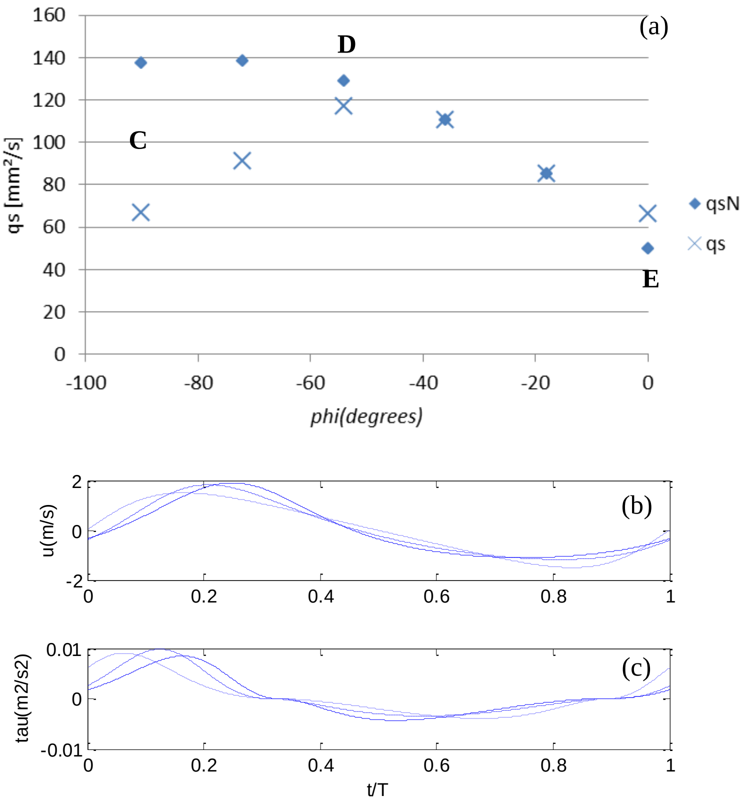

Figure 6. (a) Computed q_{sN} and q_s against ϕ; b) time series of the orbital velocity and c) bed-shear stress corresponding to **C** (solid line), **D** (dashed line) and **E** (dot-dot line).

The picture in Figure 6 is different. In this case the wave shape evolves from a non-linear first order cnoidal wave (C: $\phi = -\pi/2$) to an asymmetric and skewed wave (D: $\phi = -0.3\pi$) and, finally, to a saw-tooth wave shape (E: $\phi = 0$). The unsteady effects are already noticeable at C but, in this case, sediments entrained during the positive half-cycle do not settle and feed the transport in the negative direction. In this way, the positive net transport decreases (F is positive but lower than 1). However, this tendency tends to disappear as the wave becomes more asymmetric (D) and again for a saw-tooth wave shape the unsteadiness reinforces the transport in wave direction. The change of the wave form, as depicted in Figure 6, mimics a wave that propagates towards the shore (Ruessink *et al.*, 2011): through velocity-skewed (preponderance of short, high crests) in the shoaling zone, to velocity-asymmetric (pitched-forward, saw tooth) in the inner surf and swash zone.

5 Conclusion

In this paper a new analytical function that describes the unsteady phase-lag effects between the velocity and sediment concentration is proposed based on the previous works of Dibajnia and Watanabe (1992) and Silva *et al*. (2006). The analytical function, when effective, can modify the magnitude and also the direction of the net transport rates in non-linear waves: for skewed waves it leads to a decrease of the sediment fluxes in the wave direction, while for asymmetric pitched-forward waves it promotes sediment fluxes in the wave direction. These trends are in agreement with the experimental observations of sediment transport in non-linear waves. The application of this function to the quasi steady models of Silva *et al*. (2006) and Abreu *et al.* (2013a) provided better estimates for the net transport rates under sheet flow conditions and non-linear oscillatory flows. The lowest agreement between the numerical and the experimental results were observed for the hydraulic conditions corresponding to short wave periods (T=3s) and large orbital velocity

amplitudes that possess opposing collinear mean currents (datasets of Watanabe and Sato, 2004 and Dong *et al*., 2013) which lead to large unsteady effects. However, the plausibility of these data as representative of the near shore conditions should be questioned.
The analytical function shows a high dependence on the Shields parameter and on the values prescribed for ω_{cr}, both controlling the amount of sediments exchange between succeeding half-cycles. The description of the phase-lag effects in other semi-unsteady models (e.g., van der A *et al*., 2013) may provide better descriptions and improve the present results.

Acknowledgements

Part of this work is funded by the Research Projects PTDC/CTE-GIX/111230/2009 (EROS) and PTDC/ECM/103801/2008 (3D-MOWADI), supported by the Portuguese Foundation for Science and Technology (FCT).

References

Abreu, T., Silva, P.A., Sancho, F., Temperville, A., 2010. Analytical approximate wave form for asymmetric waves. *Coastal Engineering*, 57, pp. 656–667, doi:10.1016/j.coastaleng.2010.02.005.

Abreu, T., Michallet, H., Silva, P.A., Sancho, F., van Der A, D.A., Ruessink, B.G., 2013a. Bed shear stress under skewed and asymmetric oscillatory flows. *Coastal Engineering*, 73, pp. 1-10, doi: 10.1016/j.coastaleng.2012.10.001.

Abreu, T, Sancho, F., Silva, P.A., 2013b. Sheet-flow sediment transport formulae verification under a new set of experiments, 6th SCACR – International Short Course/Conference on Applied Coastal Research.

Bailard, J.A., 1981. An energetics total load sediment transport model for a plane sloping beach. *Journal of Geophysical Research*, 86(C11), pp. 10938–10954.

Dibajnia M., 1995. Sheet flow transport formula extended and applied to horizontal plane problems, *Coastal Eng. in Japan*, JSCE, Vol. 38(2), pp. 179-194.

Dibajnia, M., Watanabe, A., 1992. Sheet flow under non-linear waves and currents. Proc. 23rd Int. Conf. on Coastal Eng. pp. 2015–2028.

Dohmen-Janssen, C.M., 1999. Grain size influence on sediment transport in oscillatory sheet flow: phase lags and mobile bed effects. PhD thesis, Delft University of Technology.

Dohmen-Janssen, C.M., Kroekenstoel, D.F., Hassan, W.N., Ribberink, J.S., 2002. Phase lags in oscillatory sheet flow: experiments and bed load modelling. *Coastal Engineering*, 46, pp. 61–87.

Dong, L.P., Sato, S., Liu, J., 2013. A sheetflow sediment transport model for skewed-asymmetric waves combined with strong opposite currents. *Coastal Engineering*, 71, pp. 87–101, doi: 10.1016/j.coastaleng.2012.08.004.

Nielsen, P., 2006. Sheet flow sediment transport under waves with acceleration skewness and boundary layer streaming. *Coastal Engineering*, 53(9), pp. 749-758, doi:10.1016/j.coastaleng.2006.03.006.

O’Donoghue, T, Wright, S., 2004. Flow tunnel measurements of velocities and sand flux in oscillatory sheet flow for well-sorted and graded sands, *Coastal Engineering*, 51, pp.1163– 1184.

Ruessink, B.G., Michallet, H., Abreu, T., Sancho, F., van der A, D.A., van der Werf, J.J., Silva, P.A.,2011. Observations of velocities, sand concentrations, and fluxes under velocity asymmetric oscillatory flows. *J. Geophys. Res*. 116, C03004, doi:10.1029/2010JC006443.

Silva, P.A., Temperville, A., Seabra Santos, F. 2006. Sand transport under combined current and wave conditions: A semi-unsteady, practical model. *Coastal Engineering*, 53(11), pp. 897-913, doi:10.1016/j.coastaleng.2006.06.010.

Silva, P. A., Abreu, T., Michallet, H., Hurther, D., Sancho, F., 2009. Sheet flow layer structure under oscillatory flows, *Proc. 6 IAHR River, Coastal and Estuarine Morphodynamics*: RCEM 2009, Eds. C.A. Vionnet, M. H., Garcia, E.M. Latrubesse & G.M.E. Perillo, ISBN: 9780415554268, pp. 1057-1062.

Silva, P. A., Abreu, T., van der A, D.A., Sancho, F., Ruessink, B.G., Van der Werf, J.J., Ribberink, J.S. 2011. Sediment tranport in non-linear skewed oscillatory flows: the Transkew experiments. *Journal of Hydraulic Research*, 49(sup1), pp. 72-80, doi: 10.1080/00221686.2011.592681.

van der A, D.A., O'Donoghue, T. and Ribberink, J.S., 2010. Measurements of sheet flow transport in acceleration-skewed oscillatory flow and comparison with practical formulations. *Coastal Engineering*, 57(3), pp. 331-342, doi:10.1016/j.coastaleng.2009.11.006.

van der A, DA, Ribberink, J.S., van der Werf, J.J., O'Donoghue, T., Buijsrogge, R.H., Kranenburg, W.M., 2013. Practical sand transport formula for non-breaking waves and currents, *Coastal Engineering*, 76, pp. 26–42.

Watanabe A., Isobe M., 1990. Sand transport rate under wave-current action, Proc. 22nd *International Conference on Coastal Engineering*, ASCE, pp. 2495-2507.

Watanabe, A. and Sato, S. 2004. A sheet-flow transport rate formula for asymmetric, forward-leaning waves and currents. *Proceedings of the 29th International Conference on Coastal Engineering*, ASCE, Lisbon, Portugal, pp. 1703-1714.